

# Isocyanate functionalized multiwalled carbon nanotubes for separation of lead from cyclotron production of thallium-201

L. Ouni<sup>2</sup> · M. Mirzaei<sup>1</sup> · P. Ashtari<sup>1</sup> · A. Ramazani<sup>2</sup> · M. Rahimi<sup>1</sup> · F. Bolourinovin<sup>1</sup>

Received: 27 January 2016 / Published online: 20 July 2016  
© Akadémiai Kiadó, Budapest, Hungary 2016

**Abstract** Multiwalled carbon nanotubes (MWCNTs) were modified by strong oxidizing agents and were functionalized with toluene 2,4-diisocyanate, and they were used for selective separation of Tl-201 from Pb-201 (radioactive lead). The pristine and functionalized MWCNTs were characterized by Fourier transform infrared spectroscopy and scanning electron microscopy. The optimal conditions of experiment, such as pH, amount of adsorbent, and contact time were investigated. The adsorption capacity was evaluated using both Langmuir and Freundlich adsorption isotherm models. The results showed that functionalized MWCNTs have a greater potential for adsorption of lead from aqueous solution, nuclear sample, and separation of Tl-201 from Pb-201.

**Keywords** Functionalized MWCNTs · Thallous chloride radiopharmaceutical · Adsorption/desorption · Toluene 2, 4-diisocyanate · Adsorption isotherm

## Introduction

Thallium is a soft and gray metal which is distributed in trace amounts. This metal is used in electronics, detectors, high-temperature superconductors, glass industries, and pharmacy. Thallium has 25 isotopes, among them Tl-201 ( $t_{1/2} = 73$  h) decays by electron capture, and has good imaging characteristics without excessive patient radiation dose. Tl-201 radioisotope is widely used in small and non-toxic amounts in nuclear medicine for diagnosis purposes [1].

Tl-201 is one of the cyclotron products that is produced by proton bombardment of Tl-203 target. The related reaction is Tl-203 ( $n, 3p$ ) Pb-201 which decays to Tl-201 product. The chemical separation is the main step to purify Tl-201 in pharmaceutical grade which involves two steps. The first step is the separation of Pb-201 product from Tl-203 as target matrixes, passing appropriate time to decay Pb-201, and growth of Tl-201 radioisotope. The second step is the separation and purification of Tl-201 from Pb-201 solution in the isotonic chloride solution as thallous-201 chloride for medical uses.

There are several methods for separation of trace metals from solution such as precipitation [2–4], solvent extraction [5–10], ion exchange [11–14], adsorption on manganese dioxide [15], Ferrhydrite [16], Prussian blue [17], Chromium ferrocyanide gel [18], Zeolite adsorption [19], Amonium molybdo phosphate [20], Solid Phase extraction [21, 22], Magnetic solid phase extraction [23], and adsorption on nanotubes [24–33].

Among the mentioned methods and adsorbents, the carbon nanotubes cause more attraction and are called the technology of 21st century. Carbon nanotubes have several applications in electronic, composite, engineering, and separation technology. Using CNTs is a kind of solid phase

---

✉ M. Mirzaei  
mmirzaei@nrcam.org

L. Ouni  
leilaouni60@yahoo.com

A. Ramazani  
aliramazani@gmail.com

<sup>1</sup> Nuclear Science and Technology Research Institute, End of Kargar St., P.O. Box 11365-3486, Tehran, Iran

<sup>2</sup> Department of Chemistry, Faculty of Science, The University of Zanjan, University Blvd, P.O. Box 45195-313, Zanjan, Iran

extraction and has been considered as a novel adsorbent for various organic and inorganic species at their trace level. It introduces more advantages such as simplicity, easy and fast extraction time [24–29].

It has been used for preconcentration and separation of Cu [27], Cd, Mn and Ni [28], Pb, Cd [29], Cd [30], Ag, Pb [32] and Tl [31, 33].

The toxicity of Tl species highly depends on their chemical forms. Tl(III) can easily penetrate into the body and replace potassium. It is more toxic than Tl(I), Cu(II), Cd(II) and is similar to Hg(II) [5, 6, 11, 16, 18, 33, 34].

Most of CNTs-based separation methods are according to simple adsorption of metals or related ligands on CNTs. Although the reported separations are effective and applicable, due to weak forces of the adsorbent and adsorbate species, it is a desirable functional group, which acts on extraction and attaches to CNTs by covalent bonding. In this regard, we designed CNTs adsorbent bearing desired functional group for effective and selective separation of Tl-201 from Pb-201 (as parent). According to the related literature, adsorbent which carries isocyanate functional group is able to make complexes and adsorbs lead from solution selectively. Whereas, our main aim is separation of Pb-201 from Tl-201, the designed CNTs functionalized with toluene isocyanate, which is able to selectively retain Pb-201 from cyclotron radioisotope solution. The efficiency of modification is investigated by IR, SEM, and solubility test.

The extraction conditions of modified CNTs are optimized and the best buffer, pH, extraction time, and amount of adsorbent are defined. According to our protocol, the cyclotron product of Pb-201 is adsorbed on CNTs and is separated from other contaminations such as Tl-203. After appropriate time passing and growing enough of daughter Tl-201 from Pb-201 parent, Tl-201 is washed with good efficiency. At optimal conditions, the washing efficiency is more than 95 % for time intervals up to 50 min. The purity of Tl-201 product is also determined using High Pure Germanium which showed radio pharmaceutical purity.

## Experimental

### Chemicals and solutions

HNO<sub>3</sub>, Toluene, 2,4-diisocyanate, NH<sub>3</sub>, and CH<sub>3</sub>COOH were purchased from Merck (Merck, Darmstadt, Germany). Pristine MWCNTs with 7–12 nm in outer diameter, 0.5–10 μm in length, were purchased from Sigma-Aldrich Co. (USA). A stock solution of lead (1000 mg L<sup>-1</sup>) was prepared by dissolving specific amount of lead nitrate in Deionized (DI) water. The work solutions with the concentration range of 10–120 mg L<sup>-1</sup> were prepared by

dilution of stock solution. Ammonium acetate buffer solution adjusted at pH 6 was obtained by dissolving specific amounts of ammonia and acetic acid solutions (v/v 1:1). All the chemicals were of analytical grade. DI water was used for preparation of all solutions and sample washing.

### Apparatus

Fourier transform infrared spectra were recorded by using a Perkin-Elmer FT-IR Analyzer (Mattson ATI). The surface morphology of MWCNTs was observed through scanning electron microscope (SEM, Hitachi S3400N, Japan). The concentration of lead(II) ions was done by a 757VA Metrohm polarograph instrument (Metrohm, Switzerland). The solution activity was analyzed by HPGe detector (N Type, NGC 1040, DSG, Germany). The pH values of solution were adjusted by WTW pH meter (720WTW, Gemini BV, Germany).

### Purification and functionalization of MWCNTs

The functionalized MWCNTs by carboxylic acid groups were prepared according to the earlier described method [35]. Pristine MWCNTs (1 g) were dispersed in 120 mL concentrated HNO<sub>3</sub> and sonicated for 15 min in an ultrasonic bath. The suspension was refluxed with vigorous stirring at 140 °C for 3 h. After getting cold to room temperature (25 °C), the mixture was filtered through 0.45 μm porous Teflon filter paper. The functionalized MWCNTs were washed thoroughly with DI water to neutralize the solution pH (pH > 6.5). Then, the carbon nanotubes were dried in vacuum oven at 70 °C for 12 h. The functionalized MWCNTs containing COOH and oxygen groups were obtained (O-MWCNT).

### Functionalized MWCNTs with isocyanate groups

The isocyanate functionalized MWCNTs were prepared according to methods described elsewhere [36]. As the amidating agent which reacts with carboxyl groups, Toluene 2,4-diisocyanate was selected to obtain functionalized MWCNTs containing isocyanate groups (MWCNT-NCO). Figure 1 shows the functionalization of carbon nanotubes.

### Adsorption experiments

Batch adsorption experiments were performed by adding specific amounts of MWCNTs-NCO as adsorbent, to 10 mL of solution containing Pb(II) ions (10 mg L<sup>-1</sup>). The mixture was stirred vigorously on a magnetic stirrer. Then, different adsorption parameters such as pH, the amount of

**Fig. 1** Modification and functionalization of MWCNTs with COOH and isocyanate groups

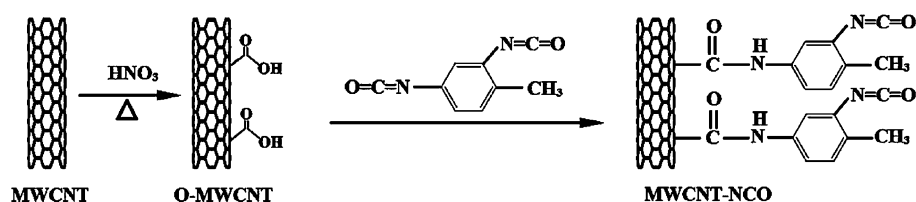
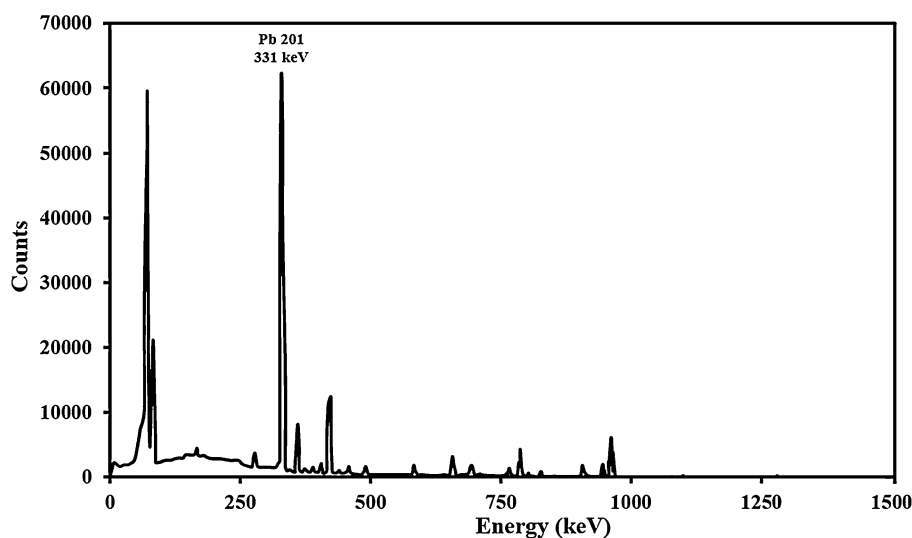


**Fig. 2** The gamma ray spectra of solution containing Pb-201 before adsorption



sorbent, and contact time were studied. The pH values of lead solutions were adjusted using  $0.1 \text{ mol L}^{-1} \text{ CH}_3\text{COOH}$  and  $\text{NH}_3$ . In all experiments before the start of experiment stages, the beaker containing MWCNTs-NCO was placed in an ultrasonic bath for 2 min. After filtration of mixture, the concentration of Pb(II) in solution was determined by polarography method. Over time, the lead ion concentration reduces due to adsorption onto functionalized MWCNTs. The adsorption percentage of Pb(II) ions is given by:

$$\% \text{Adsorption} = \frac{C_0 - C_e}{C_0} \times 100. \quad (1)$$

The amount of adsorbed Pb(II) onto the adsorbent surface (MWCNT-NCO) was calculated by the following equation [37, 38]:

$$q_e = \frac{V(C_0 - C_e)}{m}, \quad (2)$$

where  $q_e$  is the amount of Pb(II) adsorbed onto MWCNT-NCO ( $\text{mg g}^{-1}$ ),  $V$  is the initial volume of solution (L),  $C_0$  and  $C_e$  are the initial and equilibrium concentrations of Pb(II) ions in solution ( $\text{mg L}^{-1}$ ) respectively, and  $m$  is the weight of adsorbent (g).

### Adsorption of Pb-201 by MWCNT-NCO

A sample containing Pb-201 solution was added to 8 mL of buffer (pH 6). In order to study the adsorption, MWCNT-NCO was added to the solution containing Pb-201 under optimal conditions. The radioactive experiments were performed behind a lead shielding in complete safety. The initial activity of Pb-201 ions ( $28.49 \mu\text{Ci}$ ) were determined by a high purity germanium detector (HPGe) (Fig. 2). After filtering the adsorbent, the activity of solution was analyzed by HPGe detector. The difference between initial and final activities was reported as the amount of lead absorbed by MWCNT-NCO. In other words, the activity of Pb-201 was measured precisely after completion of adsorption experiments exactly, before and after filtering the adsorbent. Subsequently, the adsorption percentage was calculated using these experimental data.

### Desorption of Tl-201 (radioactive thallium)

For desorption studies, the activity of adsorbent was analyzed by an HPGe detector. The MWCNTs-NCO containing adsorbed metal ions were stirred in the range of 5–15 mL in buffer adjusted at pH 6 for 15–50 min at room

temperature. Before filtering adsorbents, the initial activity amounts of Pb-201 and Tl-201 were obtained as 2.19 and 1.48  $\mu\text{Ci}$ , respectively (Fig. 3). After filtering the adsorbent, the activity of Tl-201 and Pb-201 released in solution was measured by HPGe detector. The amount of desorption is defined as an extraction recovery ( $R$ ) of ions released from MWCNT-NCO is given by:

$$\%R = \frac{\text{Amount of ion released to solution}}{\text{Total adsorbed}} \times 100 \quad (3)$$

## Results and discussion

### FT-IR

The FT-IR spectra of pristine MWCNT, O-MWCNT, and MWCNT-NCO are shown in Fig. 4. The peaks at 1399 and 1617  $\text{cm}^{-1}$  are assigned to C=C stretching in structure of carbon nanotubes. In Fig. 4b, the broad band at 3412  $\text{cm}^{-1}$  is related to O–H stretching vibration of carboxyl groups. These peak intensities are increased in nanotubes as compared to pristine MWCNT. This difference can be explained by this fact that MWCNTs are functionalized with COOH groups. Moreover, the peaks at 1727 and 1125  $\text{cm}^{-1}$  can be attributed to C=O and C–O stretching of carboxyl groups, respectively [36]. These results indicate that the COOH group is successfully attached onto the surface of MWCNTs. In MWCNT-NCO (Fig. 4c), the broad band at 2348  $\text{cm}^{-1}$  exists due to asymmetric stretching of isocyanate groups. The bands at 1677 and 1223  $\text{cm}^{-1}$  correspond to C=O and C–N stretching of amide groups, respectively [36]. A peak is observed at around  $\approx 1544 \text{ cm}^{-1}$  which is attributed to the overlapping of a signal from the N–H and C–N bands. The bands at 2825 and 2900  $\text{cm}^{-1}$  may be due to symmetric and

asymmetric stretching vibrations of CH group at methyl groups. These results showed that functionalized carbon nanotubes containing isocyanate groups were successfully synthesized.

### SEM

The SEM images of pristine MWCNT, O-MWCNT, and MWCNT-NCO are shown in Fig. 5. As indicated in Fig. 5, the tubular structure of carbon nanotubes is well retained after functionalization. The morphology of MWCNTs shows the presence of some open ends and activated sidewalls on O-MWCNT, compared to pristine MWCNTs and suggests that the ends and sidewalls of carbon nanotubes became active [39]. The SEM image shows that the MWCNTs are covered with isocyanate group. The increase in diameter of MWCNTs indicates that the nanotubes are functionalized. Some aggregations can be detected in MWCNT-NCO micrograph because of intermolecular forces among the MWCNTs with different shapes and directions. Figure 5c clearly indicates that MWCNTs have been covered with functional groups.

### Solubility test

The solubility test of O-MWCNT was remarkably improved after functionalization. The O-MWCNTs are hydrophilic and thus could be well dispersed in water. However, MWCNT-NCO released some bubbles in contact with water. This indicates that MWCNTs-NCO are highly reactive and react in water (Fig. 6). In aqueous solution, the isocyanate group of MWCNTs-NCO reacts with water and carbamic acid is produced. Finally, the carbamic acid breaks down into amine and carbon dioxide [40].

**Fig. 3** The gamma ray spectra of solution containing Pb-201 and Tl-201 before desorption

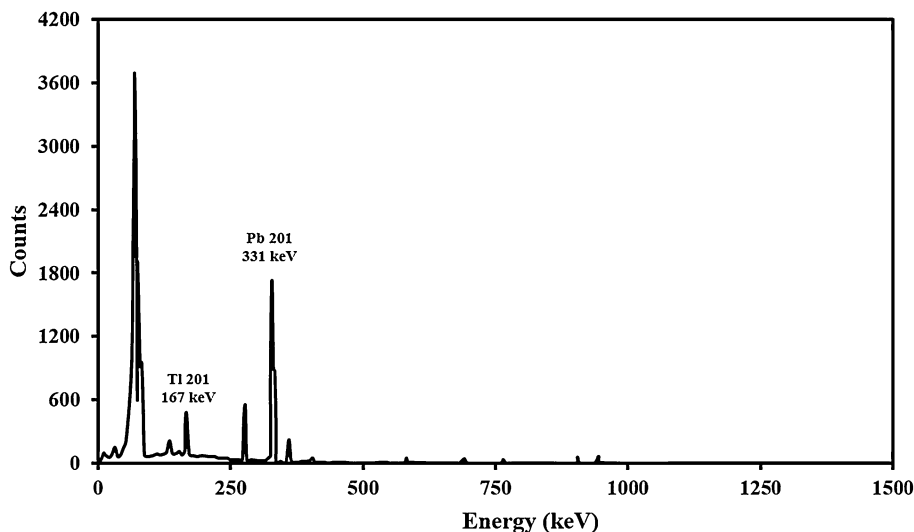
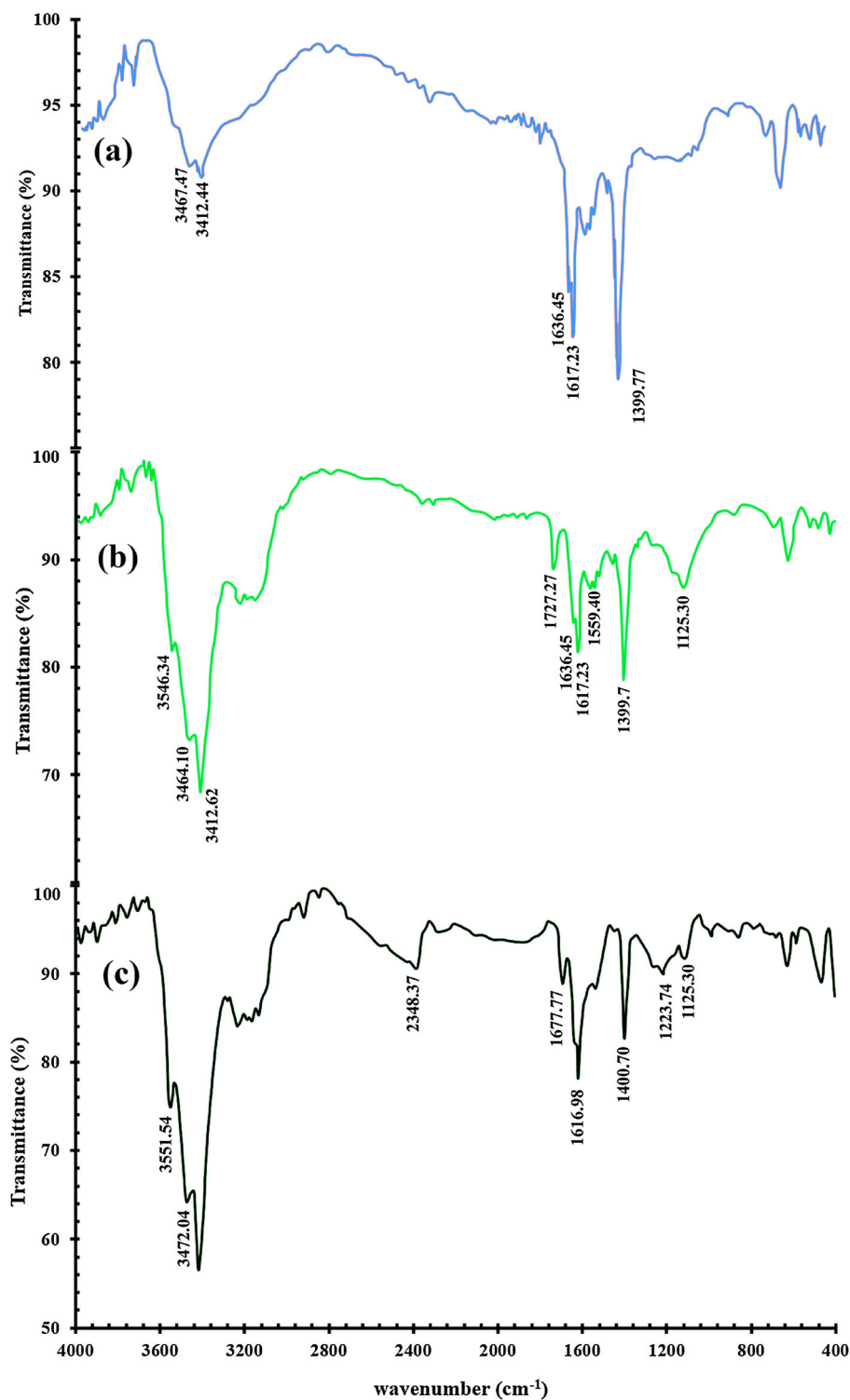


**Fig. 4** FTIR spectrum of **a** pristine MWCNT, **b** O-MWCNT and **c** MWNT-NCO

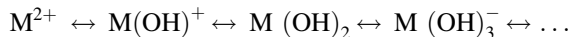


**Adsorption studies**

**Effect of pH**

The pH value is one of the most essential analytical factors in the adsorption of metal ions. There are several probable

forms of metal ions in aqueous solutions at different pH values [38, 41, 42]:



In this study, the effect of pH on lead absorption in functionalized carbon nanotubes was investigated in the range of



**Fig. 5** SEM images of **a** pristine MWCNT, **b** O-MWCNT and **c** MWNT-NCO

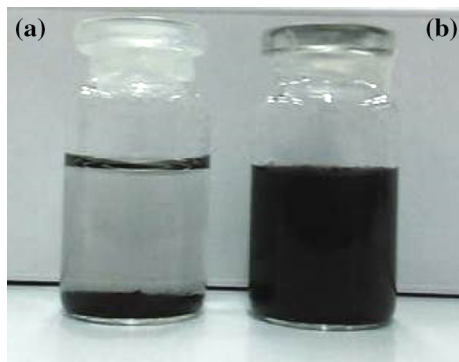


**Fig. 6** Dispersion ability of *a* pristine MWCNT and *b* O-MWCNT in water

2–8. Eventually, pH 6 was selected as the optimum pH. The results are presented in Fig. 7. In this adsorbent (MWCNT-NCO), lead adsorption level raises with increasing pH. The maximum removal of  $\text{Pb}^{2+}$  was observed at pH 6. The favorite mechanism is electrostatic interactions between metal ions (Pb) and nitrogen atoms in nanotube bed. In acidic solution ( $\text{pH} < 6$ ), where  $\text{H}_3\text{O}^+$  concentration is high, the amount of adsorption is very low due to the competition between  $\text{H}_3\text{O}^+$  and  $\text{Pb}^{2+}$  ions to interact with active sites on adsorbent. On the other hand, at low pH value, the surface of functionalized MWCNTs are covered by excess hydronium ions presence in this media. Therefore, this positive surface charge leads to high coulombic repulsion of lead ions in  $\text{Pb}^{2+}$  form and sorption sites of MWCNTs are protonated and inhibited from reaction with  $\text{Pb}^{2+}$ . As pH increased, the surface charge of MWCNTs becomes negative and consequently leads to higher adsorption of lead by MWCNTs.

A weak possible mechanism can also be considered such as the electrostatic interactions between metal ions and atoms full of electrons in nanotube surface for instance nitrogen and oxygen, electrostatic interactions between Pb(II) and nitrogen atoms of amide groups.

#### Effect of sorbent amount

The effect of sorbent amount was investigated in the range of 1–8 mg of sorbent. The adsorption of Pb(II) ions

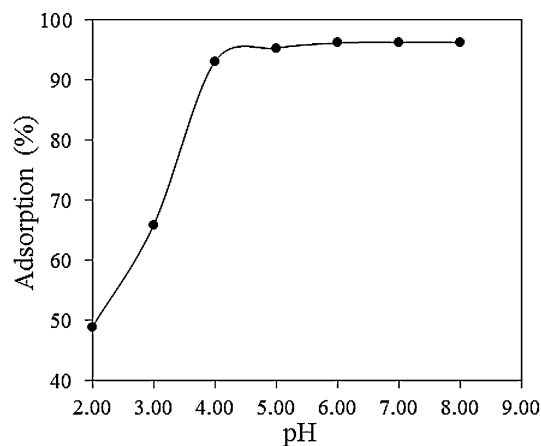


**Fig. 7** Effect of pH on the adsorption of  $\text{Pb}^{2+}$  by MWCNT-NCO.  $[\text{Pb}^{2+}]_0 = 10 \text{ mg L}^{-1}$ ,  $m_{\text{MWCNT-NCO}} = 0.005 \text{ g}$ ,  $T = 25 \text{ }^\circ\text{C}$

expanded with an increase in MWCNT-NCO mass, which could be due to the availability of more sorption sites. The results showed that 5 mg of sorbent is suitable for Pb(II) adsorption from aqueous solution (Fig. 8). Amounts of adsorbent less than 5 mg resulted in incomplete adsorption. Therefore, in all experiments, 5 mg of adsorbent was used.

#### Effect of contact time

The effect of contact time on adsorption of Pb(II) ions was studied using MWCNTs-NCO as adsorbent in the range of 5–45 min. As indicated in Fig. 9, there is a rapid increase in lead adsorption on the surface of MWCNT-NCO up to 30 min which is because of unoccupied active sites. Adsorbent reached equilibrium state after 30 min and the removal percentage remained constant. This contact time was selected for further experiments.

#### Adsorption isotherm

The equilibrium adsorption isotherms are among the basic requirements for designing adsorption systems and interaction between adsorbent and adsorbate and they could

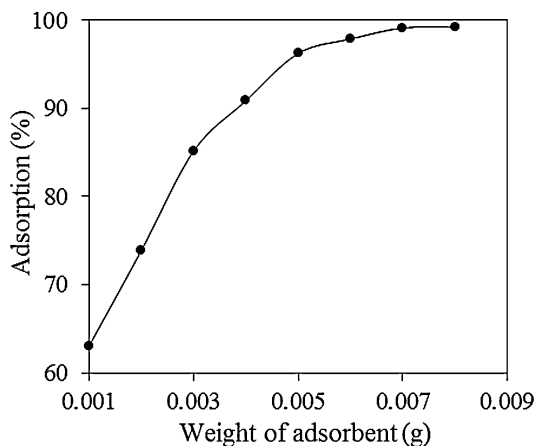


**Fig. 8** Effect of sorbent amount on the adsorption of  $Pb^{2+}$  by MWCNT-NCO.  $[Pb^{2+}]_0 = 10 \text{ mg L}^{-1}$ , pH 6,  $T = 25 \text{ }^\circ\text{C}$

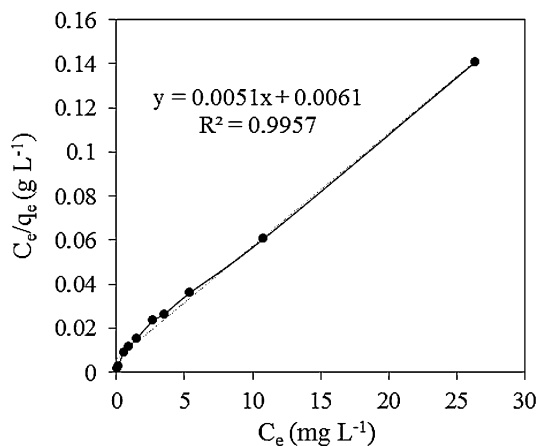


**Fig. 11** Fitting line of Langmuir adsorption isotherm of Pb(II) on MWCNT-NCO

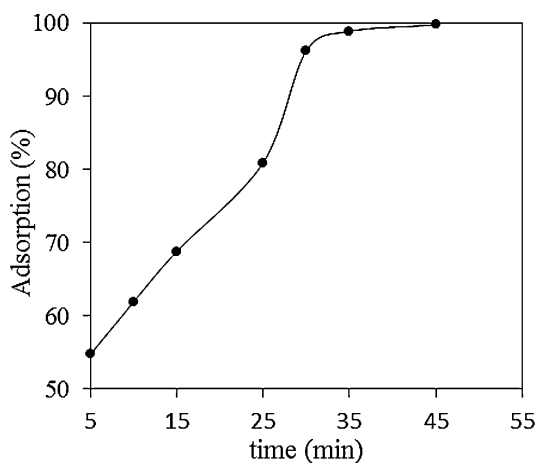


**Fig. 9** Effect of contact time on the adsorption of  $Pb^{2+}$ .  $[Pb^{2+}]_0 = 10 \text{ mg L}^{-1}$ ,  $m_{\text{MWCNT-NCO}} = 0.005 \text{ g}$ , pH 6,  $T = 25 \text{ }^\circ\text{C}$

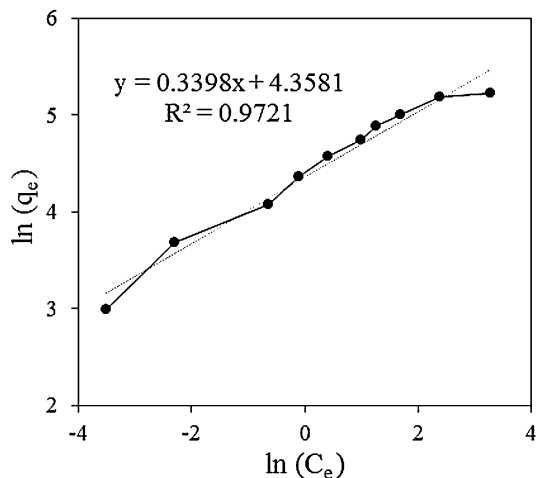


**Fig. 12** Fitting line of Freundlich adsorption isotherm of Pb(II) on MWCNT-NCO

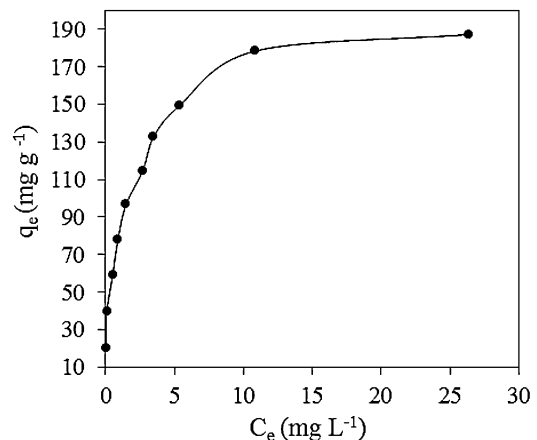


**Fig. 10** Adsorption isotherm of Pb(II) ions on MWCNT-NCO

provide the necessary information about adsorption capacity [43].

Langmuir isotherm is based on this assumption that in the maximum amount of adsorption, only one layer of adsorbate is adsorbed on surface of adsorbent and considers homogeneous surface; whereas, Freundlich model assumes that adsorption occurs on a heterogeneous adsorbent surface and in high concentrations the adsorption capacity does not remain constant. This shows a multilayer adsorption model [44–46].

The Langmuir and Freundlich models are given by the following equations, respectively:

$$q_e = q_{\text{max}} K_L C_e / (1 + K_L C_e), \tag{4}$$

$$q_e = K_F C_e^{1/n}, \tag{5}$$

where  $q_{\text{max}}$  is the maximum amount of metal ions adsorbed per unit weight of MWCNTs at a high equilibrium ion

concentration (maximum adsorption capacity) ( $\text{mg g}^{-1}$ );  $K_L$  represents the Langmuir isotherm constant which is related to the energy of adsorption ( $\text{L mg}^{-1}$ );  $K_F$  ( $\text{mg}^{1-n} \text{L}^n \text{g}^{-1}$ ) and  $n$  are Freundlich isotherm constants which are related to adsorption capacity and adsorption intensity, respectively [38]. The essential characteristic of Langmuir isotherm can be expressed by a dimensionless constant called separation factor (also called equilibrium parameter) which is defined by the following equation:

$$R_L = 1 / (1 + K_L C_0) \tag{6}$$

The value of  $R_L$  indicates the type of isotherm to be either unfavorable ( $R_L > 1$ ), linear ( $R_L = 1$ ), favorable ( $0 < R_L < 1$ ), or irreversible ( $R_L = 0$ ) [38, 47].

Equilibrium isotherm studies were carried out at lead initial concentration range of 10.0–120.0  $\text{mg L}^{-1}$  under

optimum conditions at ambient temperature. The experimental data were collected as described in the previous section and were fitted to Langmuir and Freundlich isotherm models.

As shown in Fig. 10, the experimental data fit well with Langmuir model. Figures 11 and 12 show the linearized Langmuir and Freundlich plots, respectively. Considering the slopes and intercepts of these plots, the maximum adsorption capacity and Langmuir and Freundlich constant were calculated. The  $R^2$  value of Langmuir and Freundlich models reveals that one of models fits well to experimental data. Based on correlation coefficient ( $R^2$ ), it could be concluded that the Langmuir model yields better fit to experimental data than the Freundlich adsorption isotherm. The correlation coefficient for Langmuir model ( $R^2 = 0.996$ ) is greater than that of Freundlich model ( $R^2 = 0.972$ ); this

**Table 1** Comparison of various adsorbents with this study

Adsorbents	Adsorption capacity ( $\text{mg g}^{-1}$ )	References
Chelating resin	7.38	[46]
MMWCN	9.3	[48]
Silica gel/gallic acid	12.63	[46]
Nanometer $\text{TiO}_2$ -DZ	22.5	[49]
Sulphuric acid-treated wheat bran	55.56	[50]
MWCNTs-TAA	71	[46]
MWCNT-NCO	196.08	This work

**Table 2** Langmuir and Freundlich isotherm parameters for Pb(II) adsorption on (a) pristine MWCNTs, (b) O-MWCNTs and (c) MWCNTs-NCO

Adsorbent	Freundlich model			$a_L$	Langmuir model				References
	$K_f$	$1/n$	$R^2$		$K_L$	$q_m$	$R_L$	$R^2$	
a	4.78	0.1429	0.980	–	3.71	6.71	–	0.961	[45]
b	12.80	0.2924	0.899	–	1.33	27.80	–	0.931	[45]
c	74.59	0.1856	0.972	2.43	333.33	196.10	0.03947	0.996	This work

**Fig. 13** The gamma ray spectra of solution after adsorption Pb-201 by MWCNT-NCO

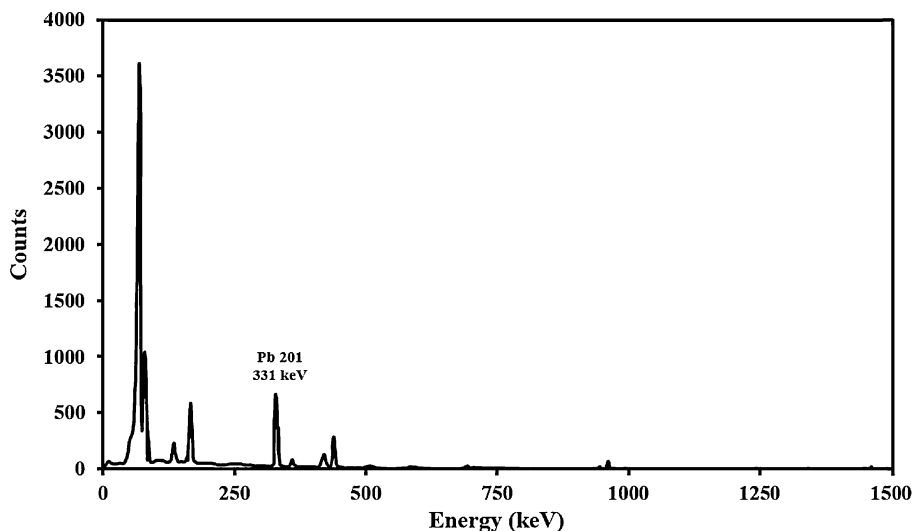
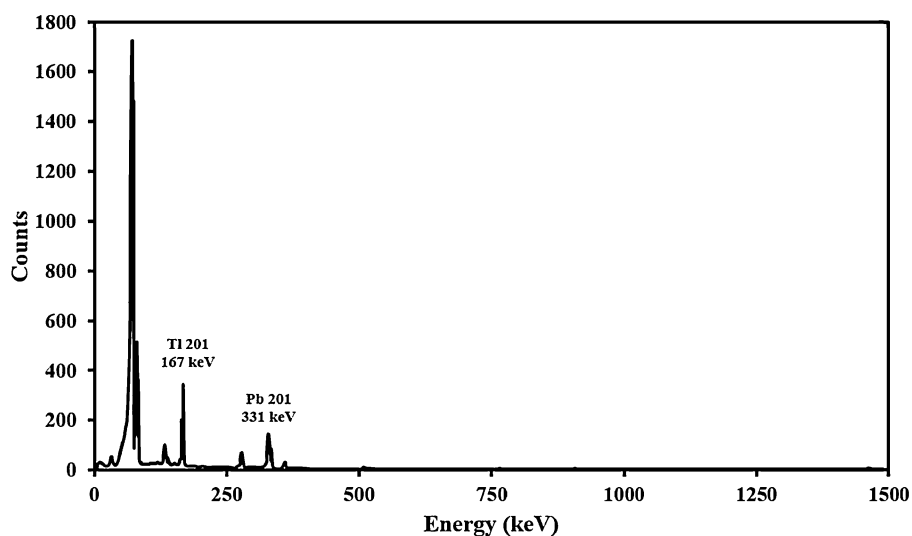




**Fig. 14** The gamma ray spectra of solution after desorption Tl-201



means that adsorption is in monolayer form. As shown in Fig. 11, Maximum adsorption capacity was found to be  $196.1 \text{ mg g}^{-1}$ . Comparison of adsorption capacity of MWCNTs-NCO with that of previous works reveals that MWCNTs-NCO can be a promising candidate for the adsorption of Pb(II) (Table 1). All isotherm parameters are listed in Table 2.

### Results of adsorption/desorption of Pb-201 on the MWCNTs-NCO

Figure 13 shows the gamma ray spectra of solution by HPGe detector after adsorption by the adsorbent. According to the present spectra, the activity of the remaining lead in solution after adsorption by MWCNT-NCO was obtained  $0.285 \text{ } \mu\text{Ci}$ . The adsorption percentage of Pb-201 was 99.00 %.

Figure 14 shows the gamma ray spectra of solution by HPGe detector after desorption process. According to the present spectra, at the optimal conditions ( $t = 50 \text{ min}$ ,  $V_{\text{detergent}} = 15 \text{ mL}$ ), the activity of Pb-201 and Tl-201 released in solution after desorption from the surface of the MWCNTs-NCO was obtained  $0.133$  and  $1.41 \text{ } \mu\text{Ci}$ , respectively. The desorption percentage of Tl-201 was 95.34 %.

### Conclusion

The attachment of COOH and NCO groups onto the surface of MWCNTs could be proved by FT-IR spectrum and SEM. MWCNTs-NCO were prepared by the reaction between toluene 2,4-diisocyanate, and carboxylated carbon nanotubes. The functionalized MWCNTs were then used

for adsorption of Pb(II) from aqueous solutions and separation of Pb-201 and Tl-201 ions.

The findings showed that the lead adsorption is dependent on solution pH, amount of adsorbent, and contact time. The Langmuir model showed better agreement with experimental data. Regarding the Langmuir equation, maximum adsorption capacity for Pb(II) with MWCNTs-NCO was  $196.1 \text{ mg g}^{-1}$ .

After the decay of Pb-201 to Tl(III)-201, the adsorbent was washed with detergent at optimal conditions and Tl(III) released into solution. The washing efficiency was more than 95 %. The results showed that MWCNTs-NCO had a high potential for adsorption of metal ions from aqueous solution, and separation of radioactive metal ions from nuclear samples. The functionalization of MWCNTs with isocyanate groups could be considered as a successful strategy for enhancing the adsorption properties of MWCNTs in removal of heavy metals from environment.

Further research works on separation of radioactive metal ions from nuclear samples by other functionalized MWCNTs in order to reach at the highest efficiency of separation.

**Acknowledgments** The authors thank the Ehsan Maadi and Sedigheh Moradkhani for carrying out Polarography and HPGe studies.

### References

- Jia YX, Lee CS, Zettl A (1994) Stabilization of the  $\text{Tl}_2\text{Ba}_2\text{Ca}_2\text{-Cu}_3\text{O}_{10}$  superconductor by Hg doping. *Phys. C* 234:24–28
- Minami C, Takei K, Funahashi T, Kubota H (1990) Recovery of high purity Thallium at sumitomo works. *Rare Met Int* 90:259–262
- Marczenko Z (1986) Separation and spectrophotometric determination of elements. *E. Horwood, Chichester*, pp 564–571

4. Luke CL (1959) Photometric determination of antimony and thallium in lead. *Anal Chem* 31:1680–1682
5. Sato T, Suzuki K, Sato K (1989) Solvent extraction of trivalent Gallium, Indium, and Thallium from hydrochloric acid solutions by an alpha-hydroxyoxime. In: *Proc Int Conf. on Sep Sci Technol*, vol 2. Ottawa, pp 539–547
6. Sato T, Sato K (1989) Solvent extraction of trivalent Aluminum, Gallium, Indium, and Thallium from hydrochloric acid solutions by an acid organophosphorus compounds. In: *Proc Int Conf. on Sep Sci Technol*, vol 2. Ottawa, pp 567–577
7. Sato T, Sato K (1992) Liquid-liquid extraction of Indium(III) from aqueous acid solutions by acid organophosphorus compounds. *Hydrometallurgy* 30:367–383
8. Sato T, Yasumura H, Mizuno Y, Nishimura T (1996) Solvent extraction of trivalent Gallium, Indium, and Thallium from hydrochloric acid solutions by TOPO and TBP. *Solvent Extr* 1:559–564
9. Sato T, Sato K, Noguchi Y, Ishikawa I (1997) Liquid-liquid extraction of trivalent Gallium, Indium and Thallium from hydrochloric acid solutions by tributyl phosphate and trioctylamine. *J Min Mat* 113:185–192
10. Sodd VJ, Scholz KL, Blue JW (1982) Separation of Thallium-201 from Lead-201 using N-benzylaniline. *J Radioanal Chem* 68:277–280
11. Albert L, Masson H (1994) Thallium extraction process. Google Patents 1994
12. Nozaki T (1956) Indirect colorimetric determination of Thallium. *J Chem Soc Jpn Pure Chem Sect* 77:493–498
13. Strelow FWE, Victor AH (1972) Quantitative separation of Al, Ga, In, and Tl by cation exchange chromatography in hydrochloric acid-acetone. *Talanta* 19:1019–1023
14. Matthews AD, Riley JP (1969) The determination of Thallium in silicate rocks, marine sediments and sea water. *Anal Chem Acta* 48:25–34
15. Means JL, Crerar DA, Borcsik MP, Duguid JO (1978) Adsorption of Co and selected actinides by Mn and Fe oxides in soils and sediments. *Geochim Cosmochim Acta* 42:1763–1773
16. Lin TS, Nriagu JO (1998) Speciation of Thallium in natural waters. In: Nriagu JO (ed) *Thallium in the environment, advances in environmental sci. and tech*, vol 29, Wiley, New York pp 31–44
17. Rauws A, Canton J (1976) Adsorption of Thallium ions by Prussian Blue. *Bull Environ Contam Toxicol* 15:335–336
18. Srivastava S, Bhattacharjee G (1980) Studies in the use of inorganic gels in the removal of heavy metals. *Water Res* 14:113–115
19. Eyde D (1993) Using zeolites in the recovery of heavy metals from mining effluents. In: Hager JP (ed) *EPD Congress '93, Proceedings EPD-TMS Annual Meeting, Denver, CO, 1993, The minerals, metals, and materials society, Warrendale, 1993*, pp 383–392
20. Zaitseva N, Deptula C, Khan K, Knotek O, Mikec P, Khalkin V (1988) Radiochemical separation of radio Thallium from proton-irradiated Lead. *J Radioanal Nucl Chem* 121:307–321
21. Yamini Y, Ashtari P, Khanchi AR, Ghanadi-Maragheh M, Shamsipur M (1999) Preconcentration of trace amounts of uranium in water samples on octadecyl silica membrane disks modified by bis(2-ethylhexyl) hydrogen phosphate and its determination by alpha-spectrometry without electrodeposition. *J Radioanal Nucl Chem* 242:783–786
22. Shamsipur M, Yamini Y, Ashtari P, Khanchi AR, Ghanadi-Maragheh M (2000) A rapid method for the extraction and separation of uranium from thorium and other accompanying elements using octadecyl silica membrane disks modified by Tri-n-octyl phosphine oxide. *Sep Sci Technol* 35:1011–1019
23. Ashtari P, Wang K, Yang X, Ahmadi SJ (2009) Preconcentration and separation of ultra-trace Beryllium using quinalizarine modified magnetic microparticles. *Anal Chim Acta* 646:123–127
24. Zheng F, Baldwin DL, Fifield LS, Anheier NC, Aardahl CL, Grate JW (2006) Single-walled carbon nanotube paper as a sorbent for organic vapor preconcentration. *Anal Chem* 78:2442–2446
25. Zhou QX, Wang WD, Xiao JP (2006) Preconcentration and determination of nicosulfuron, thifensulfuron-methyl and metsulfuron-methyl in water samples using carbon nanotubes packed cartridge in combination with high performance liquid chromatography. *Anal Chim Acta* 559:200–206
26. Zhou QX, Jp Xiao, Wang WD, Liu GG, Shi QZ, Wane JH (2006) Determination of atrazine and simazine in environmental water samples using to high performance liquid chromatography with diode array detector. *Talanta* 68:1309–1315
27. Liang P, Ding Q, Song F (2005) Application of multiwalled carbon nanotubes as solid phase extraction sorbent for preconcentration of trace copper in water samples. *J Sep Sci* 28:2339–2343
28. Liang P, Liu Y, Guo L, Zeng J, Lu HB (2004) Multiwalled carbon nanotubes as solid-phase extraction adsorbent for the preconcentration of trace metal ions and their determination by inductively coupled plasma atomic emission spectrometry. *J Anal Atom Spectr* 19:1489–1492
29. Li Y, Wang S, Luan Z, Ding J, Xu C, Wu D (2003) Adsorption of cadmium(II) from aqueous solution by surface oxidized carbon nanotubes. *Carbon* 41:1057–1062
30. Tavallali H, Fakhraee V (2011) Preconcentration and determination of trace amounts of Cd<sup>2+</sup> using multiwalled carbon nanotubes by solid phase extraction-flame atomic absorption spectrometry. *Int J ChemTech Res* 3:1628–1634
31. Pu Y, Yang X, Zheng H, Wang D, Su Y, He J (2013) Adsorption and desorption of Thallium(I) on multiwalled carbon nanotubes. *Chem. Eng J* 219:403–410
32. Tavallali H (2013) Preconcentration and determination of trace amounts of Ag(I) and Pb(II) using multiwalled carbon nanotubes by solid phase extraction-flame atomic absorption spectrometry. *Int J Chem Tech Res* 3(3):1628–1634
33. Biaduń E, Sadowska M, Ospina-Alvarez N, Krasnodebska-Ostręga B (2016) Direct speciation analysis of Thallium based on solid phase extraction and specific retention of a Tl(III) complex on alumina coated with sodium dodecyl sulfate. *Microchim Acta* 183(1):177–183
34. Rosengrant L, Craig RM (1990) Final best demonstrated available technology (BDAT) background document for P and U Thallium wastes. US EPA Office of Solid waste, Washington, p 19
35. Asadollahi N, Yavari R, Ghanadzadeh H (2015) Preparation, characterization and analytical application of stannic molybdophosphate immobilized on multiwalled carbon nanotubes as a new adsorbent for the removal of strontium from wastewater. *J Radioanal Nucl Chem* 303:2445–2455
36. Zhao C, Ji L, Liu H, Hu G, Zhang S, Yang M, Yang Z (2004) Functionalized carbon nanotubes containing isocyanate groups. *J Solid State Chem* 177:4394–4398
37. Moosa A, Ridha AM, Najem Abdulla I (2015) Chromium ions removal from wastewater using carbon nanotubes. *Int J Innov Res Sci Eng Technol* 4(2). doi:10.15680/IJIRSET.2015.0402057
38. Srivastava S (2013) Sorption of divalent metal ions from aqueous solution by oxidized carbon nanotubes and nanocages: a review. *Adv Mater Lett* 4(1):2–8
39. Kim YS, Cho JH, Ansari SG, Kim HI, Dar MA, Seo HK, Kim GS, Lee DS, Khang G, Shin HS (2006) Immobilization of avidin on the functionalized carbon nanotubes. *Synth Met* 156:938–943
40. Shimizu K, Phanopoulos C, Loenders R, Abel ML, Watts JF (2010) The characterization of the interfacial interaction between polymeric methylene diphenyl diisocyanate and aluminum: a ToF-SIMS and XPS study. *Surf Interface Anal.* doi:10.1002/sia.3586

41. Weng CH (2004) Modeling Pb(II) adsorption onto sandy loam soil. *J Colloid Interface Sci* 272:262–270
42. Sitko R, Turek E, Zawisza B, Malicka E, Talik E, Heimann J, Gagor A, Feist B, Wrzalik R (2013) Adsorption of divalent metal ions from aqueous solutions using graphene oxide. *Dalton Trans* 42:5682–5689
43. Atieh MA, Bakather OY, Tawabini BS, Bukhari AA, Khaled M, Alharthi M, Fettouhi M, Abuilaiwi FA (2010) Removal of Chromium(III) from water by using modified and nonmodified carbon nanotubes. *J Nanomater*. doi:[10.1155/2010/232378](https://doi.org/10.1155/2010/232378)
44. Ruparelia JP, Duttagupta SP, Chatterjee AK, Mukherji S (2008) Potential of carbon nanomaterials for removal of heavy metals from water. *Desalination* 232:145–156
45. Tehrani MS, Abroomand Azar P, Ehsani Namin P, Moradi Dehaghi Sh (2013) Removal of Lead ions from wastewater using functionalized multiwalled carbon nanotubes with Tris(2-Aminoethyl)Amine. *Appl Environ Prot*. doi:[10.4236/jep.2013.46062](https://doi.org/10.4236/jep.2013.46062)
46. Tehrani MS, Abroomand Azar P, Ehsani Namin P, Moradi Dehaghi Sh (2014) Removal of Lead ions from aqueous solution using multi-walled carbon nanotubes: the effect of functionalization. *J Appl Environ Biol Sci* 4:316–326
47. Bulut E, Ozacar M, Sengil IA (2008) Equilibrium and kinetic data and process design for adsorption of congo red onto bentonite. *J Hazard Mater* 154:613–622
48. Mohammadi S, Afzali D, Pourtalebi D (2010) Flame atomic absorption spectrometric determination of trace amounts of Lead, cadmium and nickel in different matrixes after solid phase extraction on modified multiwalled carbon nanotubes. *Cent Eur J Chem* 8(3):662–668
49. Lian N, Chang X, Zheng H, Wang S, Cui Y, Zhai Y (2005) Application of dithizone modified TiO<sub>2</sub> nanoparticles in the preconcentration of trace chromium and Lead from sample solution and determination by inductively coupled plasma atomic emission spectrometry. *Microchim Acta* 151:81–86
50. Ozer A (2007) Removal of Pb(II) ions from aqueous solutions by sulphuric acid-treated wheat bran. *J Hazard Mater* 141:753–758